Fault welding by pseudotachylyte formation

Thomas M. Mitchell[1], Virginia Toy[2], Giulio Di Toro[3,4,5], Jörg Renner[6], Richard H. Sibson[2]
[1]Department of Earth Sciences, University College London, WC1E 6BT London, UK
[2]Department of Geology, University of Otago, Dunedin 9054, New Zealand
[3]Dipartimento di Geoscienze, Università di Padova, 35131 Padua, Italy
[4]School of Earth and Environmental Sciences, University of Manchester M13 9PL Manchester, UK
[5]Istituto Nazionale di Geofisica e Vulcanologia, 00143 Rome, Italy
[6]Institut für Geologie, Mineralogie und Geophysik, Ruhr-Universität Bochum, 44801 Bochum, Germany

ABSTRACT

During earthquakes, melt produced by frictional heating can accumulate on slip surfaces and dramatically weaken faults by melt lubrication. Once seismic slip slows and arrests, the melt cools and solidifies to form pseudotachylytes, the presence of which is commonly used by geologists to infer earthquake slip on exhumed ancient faults. Field evidence suggests that solidified melts may weld seismic faults, resulting in subsequent seismic ruptures propagating on neighboring pseudotachylyte-free faults or joints and thus leading to long-term fault slip delocalization for successive ruptures. We performed triaxial deformation experiments on natural pseudotachylyte-bearing rocks, and show that cooled frictional melt effectively welds fault surfaces together and gives faults cohesive strength comparable to that of an intact rock. Consistent with the field-based speculations, further shear is not favored on the same slip surface, but subsequent failure is accommodated on a new subparallel fault forming on an off-fault preexisting heterogeneity. A simple model of the temperature distribution in and around a pseudotachylyte following slip cessation indicates that frictional melts cool to below their solidus in tens of seconds, implying strength recovery over a similar time scale.

INTRODUCTION

During earthquake slip on a plane or within a narrow fault zone, heat (Q) is produced in proportion to the shear stress required to cause slip (τ) and the total displacement (d). When slip is rapid and shear localized, this heat does not diffuse away from the fault plane during slip due to low thermal diffusivity of the wall rocks, and temperature increases to >1000 °C can cause selective melting (Sibson, 1975; Spray, 1992). Most experimentally generated friction-derived melts form after a critical yield strength is surpassed (Hirose and Shimamoto, 2005), but once formed, the presence of melt on the fault plane mostly causes significant reduction in frictional strength. Once faults are dynamically weakened by melt lubrication, frictional resistance is insufficient to generate the heat to drive further melt production, but the melt cools and solidifies to pseudotachylyte (PST); solidification likely leads to strength recovery and may play a role in cessation of slip. Some field studies have speculated that solidified melts may weld seismic faults (Di Toro and Pennacchioni, 2005), hindering either further seismic slip or incremental repeated slip along the same fault, causing slip to migrate to a new rupture surface in the host rock (e.g., Chester and Chester, 1998).

The geometry of PSTs has previously been used to estimate dynamic shear stress (Sibson, 1975), earthquake source parameters (Di Toro et al., 2005a, 2005b), coseismic melt pressures

(Rowe et al., 2012), and further dynamic mechanical properties (Griffith et al., 2012). However, some key questions remain: what is the strength of the fault once the melt has cooled to form a PST, and can such PSTs be reactivated during subsequent earthquakes?

We compare naturally generated fault surfaces from two major fault zones; New Zealand's Alpine fault zone (Figs. 1A and 1B) and the Gole Larghe fault zone (GLFZ), northern Italy (Figs. 1C and 1D) (Di Toro and Pennacchioni, 2005; Smith et al., 2013). The microstructural characteristics of host rocks are distinctly different in these fault systems. The foliated, micaceous Alpine fault zone mylonites are structurally heterogeneous on the millimeter scale (Fig. DR2 in the GSA Data Repository[1]). Conversely, the interlocking texture of GLFZ biotite-bearing tonalite imparts structural homogeneity at the scale of the laboratory samples (Fig. DR2). However, at outcrop scale, the GLFZ tonalite contains arrays of parallel, meter-spaced cooling joints (Pennacchioni et al., 2006, their figure 4B).

The contrast in grain-scale microstructure affects both the habit of naturally generated PST and the locus of failure in the experiments. In natural outcrops of the Alpine fault zone

mylonites we observe numerous subparallel PST layers in close proximity (Fig. 1B), and the bulk of melt-generating slip occurred on planes parallel to their foliation (fault veins; Sibson, 1975), which may indicate low and/or heterogeneous strength (Toy et al., 2011). At outcrop scale, faults in the GLFZ appear to exploit preexisting joint planes that have meter-scale spacing (Fig. 1D) and a cohesive strength lower than the wall rock due to biotite or chlorite fillings (Di Toro and Pennacchioni, 2005).

We performed triaxial deformation experiments on cores of Adamello tonalite and Alpine fault mylonite that were 30 mm in diameter and 70 mm in length. Three types of samples were prepared for each rock type: intact, sawcut, and PST bearing (Fig. 2; Fig. DR2), allowing us to compare the strength of pre-earthquake faults (sawcut) to post-earthquake faults containing solidified frictional melt, and to assess how much strength was regained relative to an intact sample. The samples were prepared with the sawcut, PST, and foliation planes orientated at 30° to the long axis of the core, the direction in which the maximum compressive stress σ_1 is applied. The plane orientations are close to the most favorable orientation for reactivation (Sibson, 1974). Details of the experiments are given in the GSA Data Repository.

EXPERIMENTAL RESULTS AND MICROSTRUCTURAL OBSERVATIONS

Multiple tests were conducted on the three sorts of samples for each rock type, at a confining pressure of 100 MPa corresponding to a depth of ~4 km. Axial strain was increased until macroscopically localized fracture associated with a stress drop and slip (intact and PST) or stable sliding on the existing fault surface (sawcut) occurred. All samples were slid for a total axial displacement of ~3 mm to establish the post-failure strength. Dynamic slip velocities and displacement during the stress drop could not be resolved in this experimental setup.

The tonalite sample with a sawcut began sliding at ~200 MPa differential stress, with the peak strength during stable sliding not higher than 300 MPa (Fig. 2A). The peak strengths of the
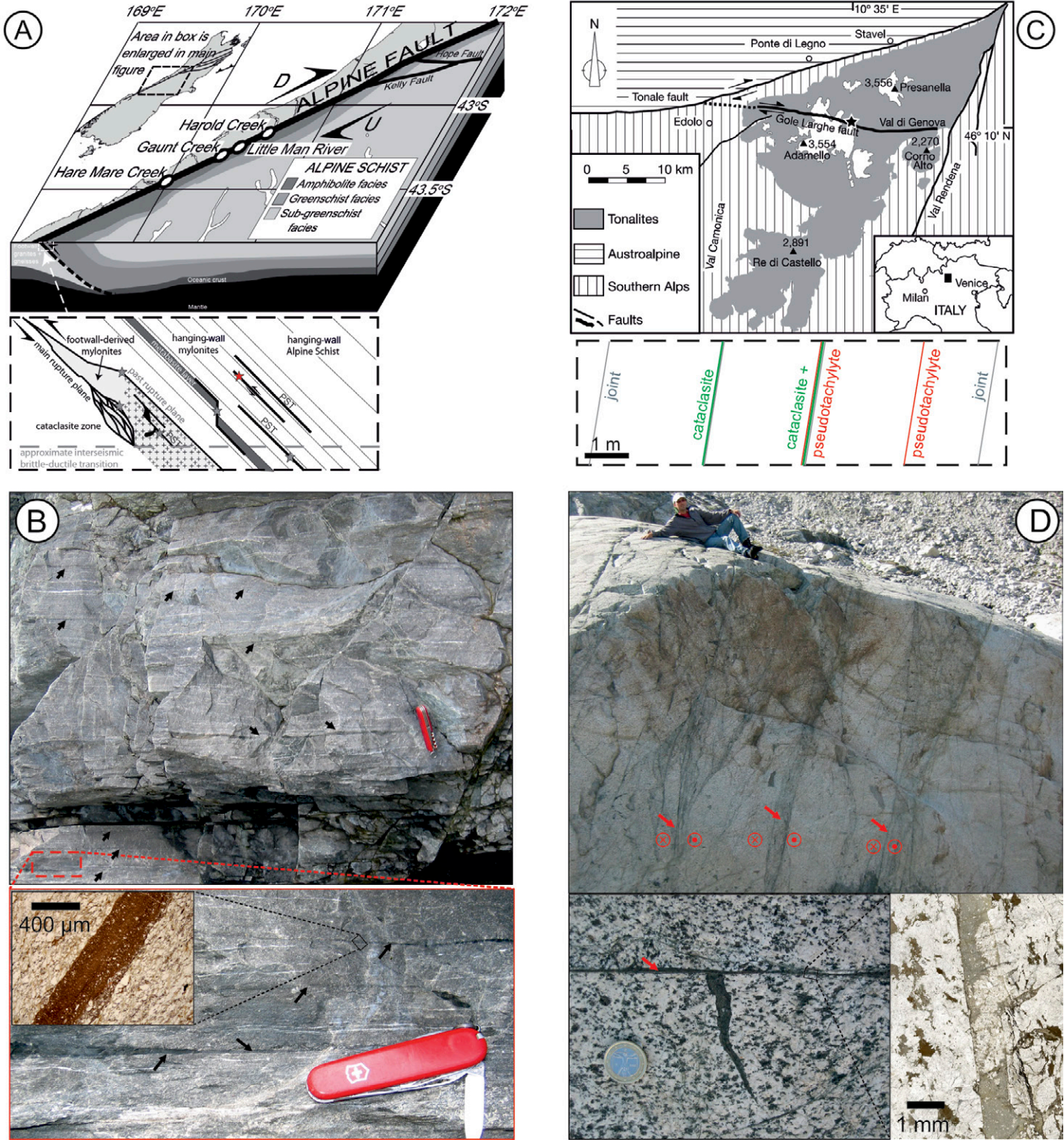

Figure 1. Sample settings. A: Block diagram and schematic vertical cross section of the Alpine fault zone, South Island, New Zealand. Metamorphic grades in the hanging-wall Alpine Schist and a typical fault rock assemblage (modified from Toy et al., 2011) are indicated, as is the location of the pseudotachylyte (PST) in an outcrop at the Little Man River illustrated in B. B: Arrows and enlargements highlight PST veins in quartzofeldspathic mylonite (photomicrograph in plane polarized light). Knife is 7 cm long. C: Map of the Adamello composite batholith and Gole Larghe fault zone (GLFZ), Italy, and schematic vertical cross section demonstrating a typical outcrop occurrence. D: Illustration of the natural setting; PSTs, cataclasites, and joints are subvertical and cut tonalites (modified from Di Toro et al., 2005a). Arrows indicate the sense of shear of the transpressive faults. An injection vein branches from the fault vein in the enlargement at center, and the second enlargement shows a plane polarized light image of the typical microstructure of the GLFZ PST.
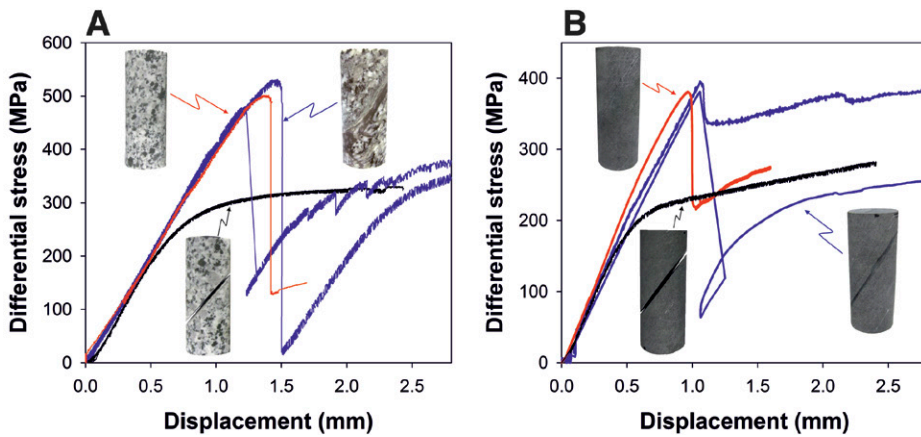
Figure 2. Differential stress-displacement plots. A: Gole Larghe, Italy, samples. B: Alpine fault zone, New Zealand, samples. Red lines represent records for intact cylinders, blue for intact cylinders containing pseudotachylytes, and black for cylinders containing sawcuts (simulated faults).

two PST-bearing faults in tonalite were significantly larger than the frictional strength of the sawcut fault, with values of ~500 MPa differential stress. These values are close to the peak strength of intact tonalite (~500 MPa; Fig. 2A) showing that the PST-bearing fault is as strong as an unfaulted intact rock. Similar results were found for the Alpine fault samples, with the sawcut sample sliding stably at ~200 MPa differential stress, and PST-bearing samples showing the same peak strength (~400 MPa) as intact, unfaulted samples (Fig. 2B). The variation in the stress drop between the two PST-bearing samples is likely due to the heterogeneity of the samples, leading to variations in fracture geometry and roughness.

Subparallel brittle fractures formed in experiments on samples from both fault zones (Fig. 3; see the Data Repository). New fractures do not exploit preexisting PST layers, but failure loci are associated with existing mechanical heterogeneities, such as the boundaries of quartz-rich layers in the mylonite. New faults in experiments are localized zones of shear, but coseismic displacement during the stress drop was not large enough to create macroscopically detectable melt. We did not investigate for melt at the asperity scale previously documented in triaxial stick-slip experiments (Brantut et al., 2016; Friedman et al., 1974) and shown to increase the post-slip strength of faults (Proctor and Lockner, 2016).

The similarity in strength exhibited by PST-bearing samples and intact samples and the observations regarding failure loci suggest that sequential coseismic faulting is accommodated on new subparallel planes initiating from off-fault preexisting heterogeneity. These heterogeneities may be defined by variations in mineralogy and/or structure in the host rock, or fracture damage imparted by previous ruptures. We therefore expect repeated failure to generate parallel PST-bearing fault surfaces, as commonly observed in nature (e.g., Di Toro and Pennacchioni, 2005; Swanson, 1992). These paired systems may therefore develop by sequential, rather than coeval, slip on the two surfaces. Many other large exposures of PST-bearing faults, such as in Maine (Swanson, 2006) and Greenland (Grocott, 1981), reveal the presence of tens to hundreds of subparallel PST-bearing faults, with the PSTs apparently recording individual, sequentially occurring slip events. However, paired PST-bearing surfaces linked by dilatational stepovers infilled with PST indicate contemporary slip for some natural examples (Swanson, 1989).

DISCUSSION AND CONCLUSIONS

To estimate the characteristic time of strength recovery, we modeled the temperature distribution in and around a PST fault vein considering cooling of a thin, infinite sheet by conduction perpendicular to its margins at temperatures commensurate with the depth of PST formation (see the Data Repository). The model predicts that the wall rock of the GLFZ PST and the vein center cool below solidus in ~5 s and ~10 s, respectively (Fig. DR3a). The walls of the even thinner Alpine fault PSTs cool below their solidus in <<1 s and the vein centers in 0.2 s (Fig. DR3b). These model predictions indicate that the natural PSTs cooled below their solidus in tens of seconds, leading to fault welding in <1 min after a seismic slip event. Combining the results of the thermal modeling with our experimental constraints on strength, we conclude that PST patches weld and strengthen faults rapidly after the cessation of coseismic slip.

Based on our experimental and microstructural observations, we propose that PST formation is not a relevant long-term weakening mechanism in crustal fault zones. Frictional melting is a known and important dynamic weakening mechanism, but the solidified PST returns the strength to that of intact samples without solidified friction-derived melt. The evolution of cohesive strength during faulting (Fig. 4) includes initial failure (stage 1), stable sliding, and generation of friction melt under stick-slip conditions, leading to weakening (stage 2). Following solidification, the fault regains strength (stage 3), causing subsequent failure to occur
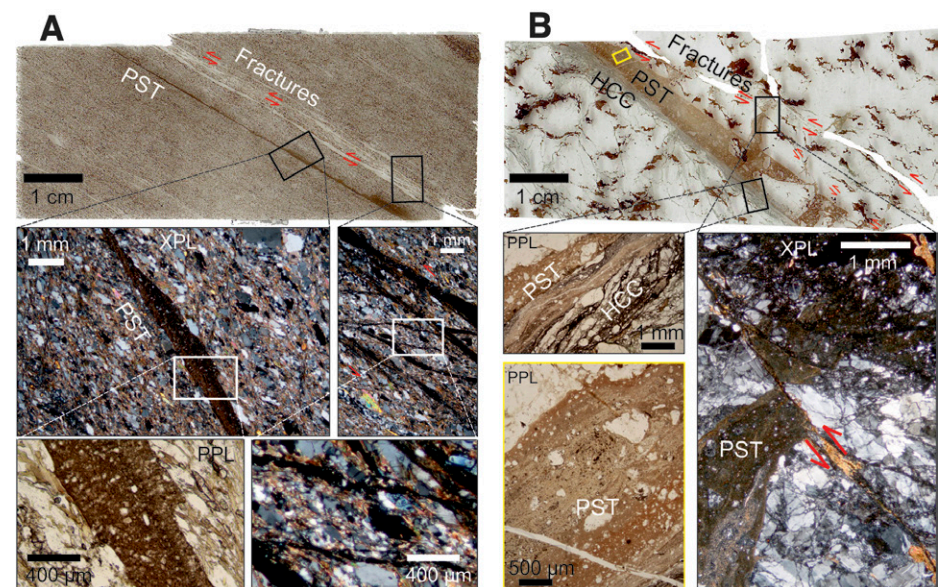

Figure 3. Microstructures of deformed samples. Top rows show scans of entire thin sections. Lower rows show photomicrographs at a variety of scales, focusing on preexisting structures on the lower left and fractures generated during the experiments on the lower right in each case. Red arrows indicate shear senses on microfaults. PST—preexisting pseudotachylyte; HCC—cataclasites; PPL—plane polarized light; XPL—cross-polarized light. A: Alpine fault zone, New Zealand. B: Gole Larghe fault zone, Italy.
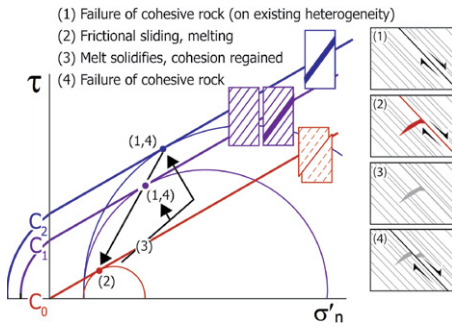
Figure 4. Synoptic illustration of the evolution of mode of failure in rocks developing pseudotachylytes (PSTs). Strength relationships are schematically indicated on a Mohr-circle diagram with a linear Coulomb envelope. C_1 and C_2 refer to the different cohesive strengths of the Alpine fault (New Zealand) mylonites and Gole Larghe fault (Italy) tonalites, respectively. Note that the cohesive strength of the intact rock is the same before generation of the PST stage 1 and after stage 4. C_0 represents both rocks when faulted and cohesionless. τ is shear stress, and σ'_n is normal stress.

on a new plane (stage 4), leaving the PST as a seismic fossil. Thus, PST formation should not generally facilitate long-term deformation localization or tectonic weakening.

The degree of PST welding along strike of a seismic fault will depend on the length scale of the PST generated along the fault. The length of PST patches varies in natural fault zones; many reported PST outcrops tend to be on the scale of centimeters to meters, but some extend for hundreds of meters to kilometers (Allen, 2005). Less commonly, some natural PST-bearing faults show localization on the boundary of the PST and wall rock, indicating seismic reactivation, where PST material is broken up and entrained into cataclastic material or a second generation of PSTs, such as in the GLFZ (Di Toro and Pennacchioni, 2005). However, such structures are not typically seen to extend over significant distances. This localization is analogous to the formation of faults at the boundaries of dikes in similar lithologic settings (e.g., d'Alessio and Martel, 2005; Pennacchioni and Mancktelow, 2007). The preexisting anisotropy of fault zone structure will have a significant effect on the evolution of coseismic slip, evolution of fault surfaces, and migration of principal slip zones over the seismic cycle.

Our experiments demonstrate that PST-bearing faults are strong under cool and dry conditions, and relatively low confining stress (i.e., upper crustal conditions). However, evidence of crystal plastic deformation of PSTs observed in nature (e.g., Passchier, 1982; Price et al., 2012) suggests that formation of PSTs may actually help to weaken lower crustal shear zones because

they commonly comprise very fine grained materials generated by devitrification or crystallized directly from hydrous melts (Toy et al., 2011), which promote grain-size–sensitive creep processes (e.g., Price et al., 2012). Thus, fault welding by PST formation is more likely in upper crustal fault zones.

REFERENCES CITED
Allen, J.L., 2005, A multi-kilometer pseudotachylyte system as an exhumed record of earthquake rupture geometry at hypocentral depths (Colorado, USA): Tectonophysics, v. 402, p. 37–54, doi: 10.1016/j.tecto.2004.10.017.

Brantut, N., Passelègue, F.X., Deldicque, D., Rouzaud, J.-N., and Schubnel, A., 2016, Dynamic weakening and amorphization in serpentinite during laboratory earthquakes: Geology, v. 44, p. 607–610, doi:10.1130/G37932.1.

Chester, F.M., and Chester, J.S., 1998, Ultracataclasite structure and friction processes of the Punchbowl fault, San Andreas system, California: Tectonophysics, v. 295, p. 199–221, doi:10.1016/S0040-1951(98)00121-8.

d'Alessio, M., and Martel, S.J., 2005, Development of strike-slip faults from dikes, Sequoia National Park, California: Journal of Structural Geology, v. 27, p. 35–49, doi:10.1016/j.jsg.2004.06.013.

Di Toro, G., and Pennacchioni, G., 2005, Fault plane processes and mesoscopic structure of a strong-type seismogenic fault in tonalites (Adamello batholith, Southern Alps): Tectonophysics, v. 402, p. 55–80, doi:10.1016/j.tecto.2004.12.036.

Di Toro, G., Nielsen, S., and Pennacchioni, G., 2005a, Earthquake rupture dynamics frozen in exhumed ancient faults: Nature, v. 436, p. 1009–1012, doi: 10.1038/nature03910.

Di Toro, G., Pennacchioni, G., and Teza, G., 2005b, Can pseudotachylytes be used to infer earthquake source parameters? An example of limitations in the study of exhumed faults: Tectonophysics, v. 402, p. 3–20, doi:10.1016/j.tecto.2004.10.014.

Friedman, M., Logan, J.M., and Rigert, J.A., 1974, Glass-indurated quartz gouge in sliding-friction experiments on sandstone: Geological Society of America Bulletin, v. 85, p. 937–942, doi:10.1130/0016-7606(1974)85<937:GQGISE>2.0.CO;2.

Griffith, W.A., Mitchell, T.M., Renner, J., and Di Toro, G., 2012, Coseismic damage and softening of fault rocks at seismogenic depths: Earth and Planetary Science Letters, v. 353–354, p. 219–230, doi:10.1016/j.epsl.2012.08.013.

Grocott, J., 1981, Fracture geometry of pseudotachylyte generation zones—A study of shear fractures formed during seismic events: Journal of Structural Geology, v. 3, p. 169–178, doi:10.1016/0191-8141(81)90012-2.

Hirose, T., and Shimamoto, T., 2005, Growth of molten zone as a mechanism of slip weakening of simulated faults in gabbro during frictional melting: Journal of Geophysical Research, v. 110, B05202, doi:10.1029/2004JB003207.

Passchier, C.W., 1982, Pseudotachylyte and the development of ultramylonite bands in the Saint-Barthelemy Massif, French Pyrenees: Journal of Structural Geology, v. 4, p. 69–79, doi:10.1016/0191-8141(82)90008-6.

Pennacchioni, G., and Mancktelow, N.S., 2007, Nucleation and initial growth of a shear zone network within compositionally and structurally heterogeneous granitoids under amphibolite facies conditions: Journal of Structural Geology, v. 29, p. 1757–1780, doi:10.1016/j.jsg.2007.06.002.

Pennacchioni, G., Di Toro, G., Brack, P., Menegon, L., and Villa, I.M., 2006, Brittle-ductile-brittle deformation during cooling of tonalite (Adamello, southern Italian Alps): Tectonophysics, v. 427, p. 171–197, doi:10.1016/j.tecto.2006.05.019.

Price, N.A., Johnson, S.E., Gerbi, C.C., and West, D.P., 2012, Identifying deformed pseudotachylyte and its influence on the strength and evolution of a crustal shear zone at the base of the seismogenic zone: Tectonophysics, v. 518, p. 63–83, doi: 10.1016/j.tecto.2011.11.011.

Proctor, B., and Lockner, D., 2016, Pseudotachylyte increases the post-slip strength of faults: Geology, v. 44, doi:10.1130/G38349.1 (in press).

Rowe, C.D., Kirkpatrick, J.D., and Brodsky, E.E., 2012, Fault rock injections record paleo-earthquakes: Earth and Planetary Science Letters, v. 335, p. 154–166, doi:10.1016/j.epsl.2012.04.015.

Sibson, R.H., 1974, Frictional constraints on thrust, wrench and normal faults: Nature, v. 249, p. 542–544, doi:10.1038/249542a0.

Sibson, R.H., 1975, Generation of pseudotachylyte by ancient seismic faulting: Royal Astronomical Society Geophysical Journal, v. 43, p. 775–794, doi:10.1111/j.1365-246X.1975.tb06195.x.

Smith, S.A.F., Bistacchi, A., Mitchell, T.M., Mittempergher, S., and Di Toro, G., 2013, The structure of an exhumed intraplate seismogenic fault in crystalline basement: Tectonophysics, v. 599, p. 29–44, doi:10.1016/j.tecto.2013.03.031.

Spray, J.G., 1992, A physical basis for the frictional melting of some rock-forming minerals: Tectonophysics, v. 204, p. 205–221, doi:10.1016/0040-1951(92)90308-S.

Swanson, M.T., 1989, Sidewall ripouts in strike-slip faults: Journal of Structural Geology, v. 11, p. 933–948, doi:10.1016/0191-8141(89)90045-X.

Swanson, M.T., 1992, Fault structure, wear mechanisms and rupture processes in pseudotachylyte generation: Tectonophysics, v. 204, p. 223–242, doi:10.1016/0040-1951(92)90309-T.

Swanson, M.T., 2006, Pseudotachylyte-bearing strike-slip faults in mylonitic host rocks, Fort Foster brittle zone, Kittery, Maine, *in* Abercrombie, R., et al., eds., Earthquakes: Radiated energy and the physics of faulting: American Geophysical Union Geophysical Monograph 170, p. 167–179, doi:10.1029/170GM17.

Toy, V.G., Ritchie, S., and Sibson, R.H., 2011, Diverse habitats of pseudotachylytes in the Alpine Fault Zone and relationships to current seismicity, *in* Fagereng, Å., et al., eds., Geology of the earthquake source: A volume in honour of Rick Sibson: Geological Society of London Special Publication 359, p. 115–133, doi:10.1144/SP359.7.